Signatures of superconductivity and pseudogap formation in nonequilibrium nodal quasiparticles revealed by ultrafast angle-resolved photoemission

Wentao Zhang (张文涛),[1] Christopher L. Smallwood,[1,2] Chris Jozwiak,[3] Tristan L. Miller,[1,2] Yoshiyuki Yoshida,[4] Hiroshi Eisaki,[4] Dung-Hai Lee,[2] and Alessandra Lanzara[1,2,*]

[1]*Materials Sciences Division, Lawrence Berkeley National Laboratory, Berkeley, California 94720, USA*

[2]*Department of Physics, University of California, Berkeley, California 94720, USA*

[3]*Advanced Light Source, Lawrence Berkeley National Laboratory, Berkeley, California 94720, USA*

[4]*Electronics and Photonics Research Institute, National Institute of Advanced Industrial Science and Technology, Ibaraki 305-8568, Japan*

(Received 3 June 2013; revised manuscript received 2 December 2013; published 30 December 2013)

We use time- and angle-resolved photoemission to measure the nodal nonequilibrium electronic states in various dopings of $Bi_2Sr_2CaCu_2O_{8+\delta}$. We find that the initial pump-induced transient signal of these ungapped states is strongly affected by the onset of the superconducting gap at T_c, superconducting pairing fluctuations at T_p, and the pseudogap at T^*. Moreover, T_p marks a suggestive threshold in the fluence-dependent transient signal, with the appearance of a critical fluence below T_p that corresponds to the energy required to break apart all Cooper pairs. These results challenge the notion of a nodal-antinodal dichotomy in cuprate superconductors by establishing a link between nodal quasiparticles and the cuprate phase diagram.

DOI: 10.1103/PhysRevB.88.245132 PACS number(s): 74.72.−h, 71.38.−k, 74.25.Jb, 78.47.jh

I. INTRODUCTION

Cuprate superconductors are known not only for extraordinarily high critical temperatures, but also for the richness of their phase diagram, where multiple energy scales associated with different electronic orders coexist at low carrier concentration and eventually merge with the critical temperature T_c at higher carrier concentration. The conventionally held wisdom is that antinodal quasiparticles shape this phase diagram.

Indeed, in conventional superconductors the energy gap and the low-energy quasiparticle spectral weight (i.e., the area under the quasiparticle peak) are virtually isotropic around the normal state Fermi surface. In contrast, in high-T_c cuprate superconductors the gap exhibits four nodes along the Brillouin-zone diagonals (nodal direction), and the quasiparticle spectral weight is strongly momentum-dependent.[1] For example, while the quasiparticle peak in underdoped cuprates exists both above and below T_c along the nodal direction, it only appears below T_c along the antinodal direction.[2] This anisotropic character is assumed to derive from the "d-wave" symmetry of the superconducting state. Because of this sensitivity to T_c, the antinodal quasiparticle excitations have been regarded as carrying the information of superconductivity. In harmony with this notion, it has been shown that the antinodal quasiparticle spectral weight scales with the critical temperature,[3–6] and recently it has been shown that this same spectral weight is also linked to the onset of superconducting pair fluctuations at T_p.[7] This dichotomous behavior between nodal and antinodal quasiparticles persists even above the critical temperature, in the so-called pseudogap phase, up to T^*.

Despite their central role in controlling most of the low-energy properties of cuprate superconductors, the role of nodal quasiparticles in superconducting transitions and more generally in shaping the cuprate phase diagram is still unclear and generally considered negligible.[8–11] This view has been challenged by a time- and angle-resolved photoemission experiment (trARPES) showing that nodal quasiparticles also respond to the superconducting transition and their spectral weight scales with the superfluid density,[12] and by the report of a nodeless energy gap in a very weakly doped sample.[13]

Here, we use trARPES to investigate changes in the nodal electron dynamics across a range of dopings and temperatures in the phase diagram of $Bi_2Sr_2CaCu_2O_{8+\delta}$ (Bi2212). We found that the initial pump-induced nodal quasiparticle population exhibits sharp features reflecting the opening of the pseudogap at T^* and the onset of superconductivity at T_c, as well as an intermediate feature at T_p, between T^* and T_c. Below T_p, fluence-dependent measurements reveal a critical fluence that corresponds to the energy required to break apart all Cooper pairs, suggesting that T_p is the onset temperature below which electrons begin to pair incoherently, and that it is distinct from T^*, which marks the onset of an independent electronic order. The present work is a demonstration that all three of these characteristic temperatures affect the dynamics of nodal quasiparticles, and not just the dynamics of antinodal quasiparticles.

II. EXPERIMENT

In our trARPES experiments,[14] an infrared pump laser pulse ($h\nu = 1.48$ eV) drives the sample into a nonequilibrium state, which is probed by an ultraviolet laser pulse ($h\nu =$ 5.93 eV) with a repetition rate 543 kHz. The beam spot size [full width at half-maximum (FWHM)] of the pump and probe are ∼100 and ∼40 μm, respectively. The delay time (t) between pump and probe pulses is controlled using a translation stage that varies the path length of the pump. For $t < 0$, the probe pulse arrives before the pump pulse, corresponding to an equilibrium measurement. For $t > 0$, the probe pulse arrives after the pump pulse, corresponding to a nonequilibrium measurement. The time resolution (∼300 fs) and $t = 0$ are determined by the cross-correlation of the pump and probe pulses as measured on polycrystalline gold with a 0.4 eV kinetic energy window centered 1.1 eV above the Fermi level. The system is equipped with a Phoibos 150 mm hemispherical electron energy analyzer (SPECS). The total

energy resolution in the experiments is ∼22 meV, and the momentum resolution is ∼0.003 Å^{-1} at the Fermi energy.

Single-crystal samples from four different dopings of Bi2212 were measured: underdoped samples with $T_c = 78$ K (UD78K) and $T_c = 84$ K (UD84K), a nearly optimally doped sample with $T_c = 91$ K (OP91K), and an overdoped sample with $T_c = 84$ K (OD84K). We also measured an overdoped sample of $Bi_{1.7}Pb_{0.4}Sr_{1.6}CuO_{6+\delta}$ (Bi2201) with $T_c = 32$ K. All single crystals were grown by the traveling solvent floating zone method. The underdoped samples were obtained by annealing the optimally doped sample in nitrogen. The overdoped Bi2212 sample was obtained by annealing the optimally doped sample in oxygen. All the samples were cleaved *in situ* in vacuum with a base pressure less than 5×10^{-11} Torr. In the temperature-dependent measurements, the samples were cleaved at temperatures at or above 25 K to minimize the sample surface aging effect caused by degassing of the cryostat when heated around 20 K.

III. QUASIPARTICLE DYNAMICS

Figure 1 shows results for the UD78K sample. At a base temperature of 20 K, the equilibrium spectrum ($t = -1.2$ ps) shows a well-known dispersion kink at binding energy $\hbar\omega_0 \approx 70$ meV as marked by the arrow in Fig. 1(a).[15] As the pump pulse strikes the sample ($t = 0$ ps), the intensity of the ARPES spectrum between the Fermi level and the kink energy is suppressed. It returns to the equilibrium value after 20 ps. Such evolution of the transient ARPES spectrum is similar to that of optimally doped Bi2212 as reported in Refs. 12 and 16. To illustrate the recovery process, Fig. 1(b) shows the change in integrated ARPES intensity above E_F [ΔI_e, see the hatched region in Fig. 1(a)], with the response at different fluences normalized to the same amplitudes. In the superconducting state, the recovery rate of the nonequilibrium state increases linearly with fluence [Fig. 1(c)] in a manner similar to that observed in optimally doped Bi2212,[16] suggesting bimolecular recombination.[17,18] As the fluence approaches a critical fluence F_c (∼13 μJ/cm^2), the decay rate undergoes a change in slope, marking the onset of different recombination processes for quasiparticles. A similar but higher critical fluence was found in a time-resolved optical reflectivity study;[19] the difference in thresholds may be because reflectivity measurements probe more of the bulk than ARPES. Such a fluence threshold is consistent with an observation of the full closure of the superconducting gap at a similar critical fluence in optimally doped Bi2212,[20] and thus we identify it as the likely fluence where all Cooper pairs have been destroyed. The identification is also consistent with a simple back-of-the-envelope calculation of the fluence needed to break apart all Copper pairs. Indeed, using a superconducting coherence length of ∼15 Å (Ref. 21) and a penetration depth of ∼100 nm (Ref. 22) (for 1.48 eV photons) in Bi2212, at F_c the laser deposits ∼0.25 meV/Å^2 of energy in the top copper oxygen plane, or ∼55 meV per coherence area. This is on the order of the energy gap in Bi2212. We note that a portion of the pulse energy may be transferred to phonons in the initial response, but it should not significantly affect our estimation because the initial nonthermal relaxation is dominated by electron-electron scattering.[23] Hence at the critical fluence the laser deposits just enough energy to completely break all Cooper pairs.

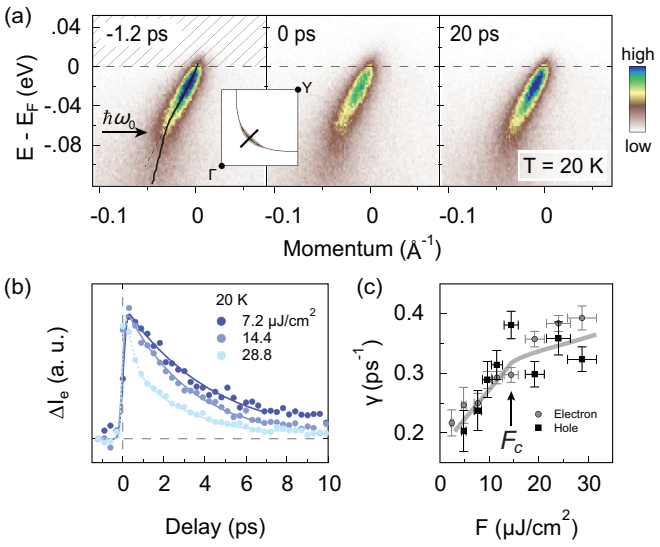

FIG. 1. (Color online) Dynamical evolution of time-resolved ARPES spectra along a nodal cut [Γ(0, 0) – Y(π, π) direction] of underdoped Bi2212 ($T_c = 78$ K). (a) ARPES dispersions: at delay time −1.2, 0, and 20 ps measured at 20 K with pump fluence 14.4 μJ/cm^2. The black solid curve represents the equilibrium electronic dispersion. (b) Electronlike quasiparticle recombination dynamics for different pump fluences at 20 K. The ΔI_e is obtained by integrating photoemission intensity across the hatched area shown in (a) and then subtracting the integral of the equilibrium intensity. Decay curves are normalized to the same amplitudes. (c) The nonequilibrium quasiparticle decay rate as a function of pump fluence (F) for both electron and hole parts at 20 K.

As the temperature increases, thermally excited quasiparticles begin to dominate the recombination dynamics,[17] making it harder to isolate the contribution of photoexcited nonequilibrium quasiparticles. This limitation can be overcome by looking at the signal at $t = 0$ (averaged over ∼300 fs because of time resolution), as the thermally excited quasiparticle have only a negligible impact on the initial excited population. The temperature-dependent nonequilibrium quasiparticle population at $t = 0$ is studied in the following section.

IV. FLUENCE AND TEMPERATURE DEPENDENCE

Figure 2 shows $\Delta I_e(t = 0)$ as a function of fluence and temperature for an underdoped sample. Two distinct regimes can be identified from the data: a high-temperature regime, which extends from the normal state [panel (a)] well into the pseudogap state [panel (b), $T^* \approx 220$ K,[24,25] where ΔI_e is linear in fluence and extrapolates to 0 at $F = 0$ (see dashed lines)]; and a low-temperature regime, which sets in above T_c [panels (b) and (c)] and persists into the superconducting state [panel (d)], where ΔI_e is clearly not linear in fluence, with high fluence values of ΔI_e extrapolating to a positive y-intercept at $F = 0$. The departure from linearity at low temperature occurs at the critical fluence ($F_c = 13 \pm 3$ μJ/cm^2) identified in Fig. 1(e). According to the interpretation that F_c marks the

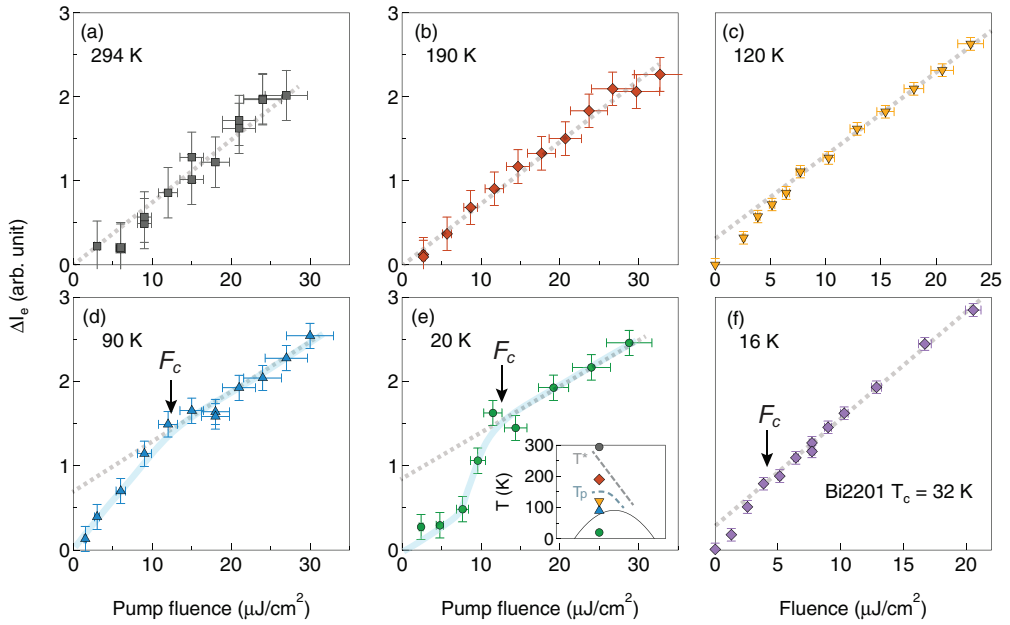

FIG. 2. (Color online) Nodal fluence dependence of the initial quasiparticle excitation density at $t = 0$ in underdoped Bi2212 ($T_c = 78$ K). (a) ΔI_e at a delay time of 0 ps measured at 294 K. (b)–(e) Same as (a) but measured at equilibrium temperature 190, 120, 90, and 20 K. As indicated in the inset of (d), the measurements correspond to equilibrium temperatures above T^* (294 K), slightly below T^* (190 K), slightly above T_c (90 K), and far below T_c (20 K). (f) Similar measurement on an overdoped Bi2201 sample ($T_c = 32$ K) at $T = 16$ K. The bold lines are guides to the eye, and the dashed bold lines are linear fits to the high fluence data. The black arrows mark the critical fluence where the slope of the curves changes.

threshold above which no Cooper pairs exist, we observe a slight decrease of F_c from 13 μJ/cm^2 [panels (d) and (e)] to 8 μJ/cm^2 as the temperature increases to 120 K [panel (c)]. Also, in a single-layer Bi2201 sample, we observe a lower F_c by a factor of 3 [panel (f)]. These observations are consistent with the interpretation of F_c and the fact that it should scale with the pairing strength, which gets weaker at higher temperatures, and is weaker in Bi2201 than in Bi2212. However, the observation of two distinct temperature regimes in the UD78K sample hints at an intermediate temperature scale between T_c and T^*, which, given the similar dynamics to that in the superconducting state, is likely related to the onset of superconducting fluctuations. In line with this observation, a recent ARPES experiment has shown that the antinodal spectral function is sensitive to the onset of superconducting pairing fluctuations at an intermediate temperature scale between T_c and T^*.[7]

In Fig. 3 we show the detailed temperature and doping dependence of ΔI_e at $t = 0$ for a fixed pump fluence (14.4 μJ/cm^2, slightly above the critical fluence). We note that the reflectance of Bi2212 has little temperature dependence from 4 to 300 K at a photon energy of 1.48 eV (variation is less than 1%),[26] guaranteeing that the pump fluence applied on the sample is unchanged during the temperature-dependent measurements. A common feature to all the dopings is a sharp step in ΔI_e at T^*, which coincides with the pseudogap temperature determined from transport experiments[24] and from momentum-resolved experiments looking at antinodal quasiparticles.[7,25] The sharp step is still observed above T_c for an overdoped sample [Fig. 3(d)], suggesting that the pseudogap temperature T^* can be defined even for

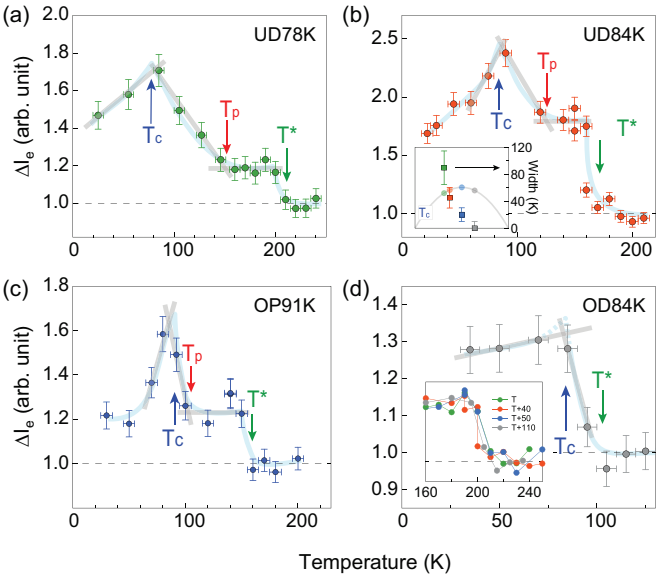

FIG. 3. (Color online) Nodal temperature dependence of the initial quasiparticle excitation density at a fixed fluence of 14.4 μJ/cm^2 for various dopings of Bi2212. (a) Underdoped ($T_c = 78$ K) sample. ΔI_e at zero delay time, defined as in Fig. 1, and normalized to the height above T^*. (b)–(d) Same as (a) for an underdoped $T_c = 84$ K sample, an optimally doped $T_c = 91$ K sample, and an overdoped $T_c = 84$ K sample. The bold cyan lines are guides to the eyes. ΔI_e at different temperature are normalized to the same probe fluence. Inset in (b) shows the width of the peaklike feature around T_c as a function of doping. Inset in (d) is ΔI_e vs temperature for the four dopings of the sample, which are scaled to the same amplitudes at T^*. Error bars are taken to be the maximum $|\Delta I(t)|$ for $t < 0$.

this overdoped sample, consistent with recent reports by equilibrium ARPES on antinodal quasiparticles.[13,25] The step indicates that nonequilibrium electronic states below T^* result in a larger contribution to ΔI_e at the node, even though there is no gap at the node itself, as is generally believed.

For the underdoped and optimally doped samples [panels (a)–(c)], further cooling reveals a distinctive peaklike feature in ΔI_e centered at T_c, and a plateau in ΔI_e above T_c that is bounded on the high-temperature side by T^* and on the low-temperature side by a temperature T_p, defined as the temperature below which ΔI_e begins to rise. The peaklike feature at T_c is reminiscent of a variety of observables that diverge in the vicinity of T_c as a result of phase fluctuations. These include, but are not limited to, λ-shaped anomalies in the temperature dependence of thermal expansivity coefficients in YBCO,[27] and a theoretical divergence of relaxation time at the critical temperature in random-field Ising systems.[28] Thus it is reasonable to infer that the peak in ΔI_e around T_c is a measure of phase fluctuations. Further confirmation comes from the sharpening of the peak as the doping increases, reflecting a narrowing of the Ginzburg window[29] [see the width of this peaklike feature as a function of doping in the inset of Fig. 3(b)]. If the peak at T_c is associated with the presence of superconducting phase fluctuations, then T_p, the end of the peak feature, should be identified with the onset of such fluctuations. This scenario is further supported by the good agreement with the Nernst effect temperature,[30] identified as the onset of superconducting fluctuations in cuprate superconductors, and the T_p measured in this experiment is along the nodal direction. The absence of T_p in the overdoped sample [panel (d)] implies that the superconducting transition is determined by Cooper pair formation rather than phase fluctuations. The nonequilibrium spectra in Figs. 3(a) and 3(b) do not saturate at the lowest temperature in our measurements for the two underdoped samples, indicating that fluctuating uncondensed pairs exist farther below T_c than on the overdoped side. Our result also demonstrates that below T_p, the breaking of uncondensed Cooper pairs by pumping dominates ΔI_e at $t = 0$.

The features at T_c, T_p, and T^* follow distinct trends as a function of doping. For all dopings, fitting the rise of the step at T^* using an error function yields a temperature smearing less than 10 K [inset of panel (d)]. The abrupt onset at T^* is reminiscent of time-resolved reflectivity measurements on Bi2201, where a similar behavior was associated with T^*, marking the onset of a phase transition.[31] The fact that ΔI_e at $t = 0$ shows the same critical fluence in both the superconducting state and between T_c and T_p [Figs. 2(c)–2(d)] demonstrates that the response of the electronic state to the pump pulse between T_p and T_c is similar to that in the superconducting state. In contrast, the absence of a critical fluence above T_p in Fig. 2 shows the different response between states below T_p and states below T^*, indicating the different underlying interactions of the pseudogap and the superconducting state.

We note that the step at T^* and the peaklike feature at T_c cannot be attributed to thermal effects. Indeed, in a thermal model the initial nonequilibrium electron population ΔI_e^{simu} is proportional to the energy integral of a Fermi-Dirac distribution between the chemical potential and infinity, which

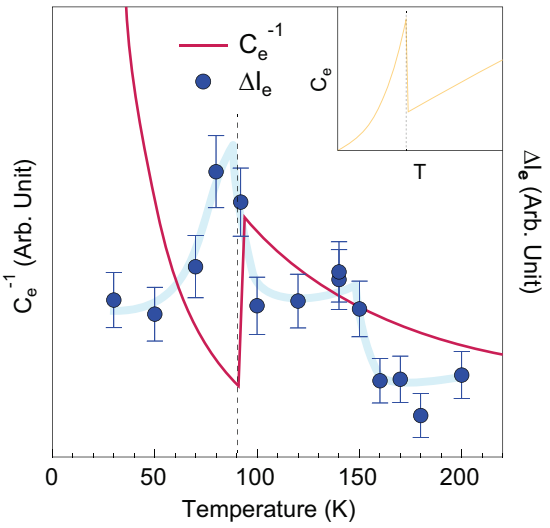

FIG. 4. (Color online) Comparison between initial nonequilibrium electrons ΔI_e and simulated electron heat capacity C_e as a function of temperature. The inset shows C_e as a function of temperature in a superconductor.

is in turn proportional to the electronic temperature T_e:

$$I_e^{\text{simu}} \propto \int_0^{+\infty} \frac{1}{e^{\omega/k_B T_e}+1} d\omega \tag{1}$$

$$\propto k_B T_e \int_0^{+\infty} \frac{1}{e^{x}+1} dx \tag{2}$$

$$\propto T_e. \tag{3}$$

It immediately follows that the change in the electronic spectral weight (ΔI_e) is proportional to the change of electronic temperature ΔT_e and independent of the equilibrium temperature.

If one assumes that the energy of the pump pulse ΔQ is mainly absorbed to heat the electrons,[23] then

$$dQ = dT_e C_e, \tag{4}$$

where C_e is the electronic heat capacity. According then to Eqs. (1)–(3), we expect that ΔI_e is inversely proportional to the specific-heat capacity C_e. In Fig. 4 we use a simple model to simulate the electron heat capacity C_e with $C_e = AT^3$ below T_c and $C_e = BT$ above T_c (A and B are constants). The direct comparison between C_e and ΔI_e shown in Fig. 4 clearly shows that the initial spectral gain above the Fermi level cannot be attributed to a simple thermal effect. Indeed, while the experimental value of $\Delta I_e(t)$ shows a peaklike feature around T_c, the model predicts a dip in C_e^{-1} at the same temperature. The basic shape of this dip feature at T_c is robust, even after integrating Eq. (4) to account for realistically finite values of ΔI_e and ΔT_e.

V. PHASE DIAGRAM AND DISCUSSION

In Fig. 5, we summarize the temperatures identified for the nodal transient spectra T_c, T^*, and T_p in the form of a phase diagram, and we compare them with similar temperature scales reported in the literature. The most important implications of this comparison are (i) the position of the peaklike feature (T_c node) in Fig. 3 matches the superconducting critical temperature T_c measured by SQUID; (ii) T_p node

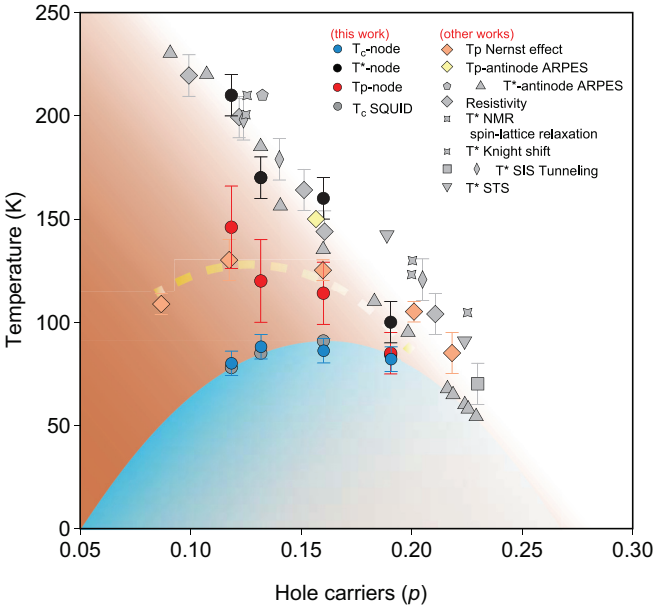

FIG. 5. (Color online) Nodal phase diagram of Bi2212. The superconducting critical temperature T_c node, superconducting fluctuation onset temperature T_p node, and pseudogap temperature T^* node of the four different dopings are plotted. T_c node (blue filled circles), T^* node (black filled circles), and T_p node (red filled circles) are determined by the transition and onset temperature in Fig. 3; T_c (gray filled circles) is derived from SQUID measurements. T_p from Nernst signal measurements (pink diamonds),[30] and off-nodal ARPES measurement (yellow diamond)[7] as well as T^* (gray data points) from ARPES,[7,25] resistivity,[24] nuclear spin-lattice relaxation,[32] the Knight shift,[32] SIS tunneling.[33,34] and STS,[35] are also plotted. The hole carrier concentration p of each sample is calculated by the Presland-Tallon equation $T_c/T_c^{\max} = 1 - 82.6(p - 0.16)^2$.[36]

coincides with the onset temperature of superconducting phase fluctuations measured by the Nernst effect;[30] and (iii) T^* node coincides with the pseudogap temperature extracted from various momentum-integrated probes[24,32–35] and from ARPES along the antinodal direction (T^* antinode).[7,13,25] The obtained phase diagram is consistent with a theoretical predication.[37]

Revealing the presence of these energy scales in the spectral function of ungapped quasiparticles disrupts the conventional view that T_c, T_p, and T^* are only associated with gapped antinodal states. The signature at T^* is perhaps the most surprising of these, as the most popular explanation for the pseudogap phase at present is that it is associated with the onset of charge ordering with a nesting vector along the $(\pi,0)$ direction, resulting, therefore, in strongly suppressed antinodal electronic states.[38] The signatures of T^* and T_c in the (π,π) direction may indicate that the gapped antinodal nonequilibrium quasiparticles in both of the pseudogap and superconducting states can be scattered to the nodal region via exchanging a momentum with other excitations in a very short time scale. Theoretical and experimental studies seems to argue against this possibility as this type of scattering is predicted to be pair-breaking,[39–41] leaving a far more exciting possibility, namely that nodal electronic states intrinsically play the same role in shaping the pseudogap and superconducting states on the phase diagram as generally believed in antinodal states.

In summary, we have revealed a strong response of nonequilibrium nodal ungapped quasiparticles to both the superconducting and pseudogap states. A phase diagram for nodal quasiparticles results from these data, similar to the one widely discussed for gapped antinodal quasiparticles, where the pseudogap temperature T^* gradually merges with the superconducting transition temperature on the overdoped side of the phase diagram, and an intermediate temperature scale T_p associated with uncondensed Cooper pairs sets in between T_c and T^*. These results highlight the important role that nodal quasiparticles play for cuprate superconductivity, as well as the different electronic natures of the pseudogap and superconducting transition.

ACKNOWLEDGMENTS

We thank J. Orenstein, S. Kivelson, and P. Phillips for useful discussions, and J. S. Wen, J. Zhao, and R. J. Birgeneau for SQUID measurements. This work was supported by Berkeley Lab's program on Quantum Materials, funded by the US Department of Energy, Office of Science, Office of Basic Energy Sciences, Materials Sciences and Engineering Division, under Contract No. DE-AC02-05CH11231.

*alanzara@lbl.gov

[1] Z.-X. Shen and J. R. Schrieffer, Phys. Rev. Lett. **78**, 1771 (1997).
[2] M. Norman, H. Ding, M. Randeria, J. Campuzano, T. Yokoya, T. Takeuchi, T. Takahashi, T. Mochiku, K. Kadowaki, P. Guptasarma *et al.*, Nature (London) **392**, 157 (1998).
[3] A. G. Loeser, Z.-X. Shen, M. C. Schabel, C. Kim, M. Zhang, A. Kapitulnik, and P. Fournier, Phys. Rev. B **56**, 14185 (1997).
[4] A. V. Fedorov, T. Valla, P. D. Johnson, Q. Li, G. D. Gu, and N. Koshizuka, Phys. Rev. Lett. **82**, 2179 (1999).
[5] D. L. Feng, D. H. Lu, K. M. Shen, C. Kim, H. Eisaki, A. Damascelli, R. Yoshizaki, J.-i. Shimoyama, K. Kishio, G. D. Gu, S. Oh, A. Andrus, J. O'Donnell, J. N. Eckstein, and Z.-X. Shen, Science **289**, 277 (2000).
[6] H. Ding, J. R. Engelbrecht, Z. Wang, J. C. Campuzano, S.-C. Wang, H.-B. Yang, R. Rogan, T. Takahashi, K. Kadowaki, and D. G. Hinks, Phys. Rev. Lett. **87**, 227001 (2001).
[7] T. Kondo, Y. Hamaya, A. D. Palczewski, T. Takeuchi, J. S. Wen, Z. J. Xu, G. Gu, J. Schmalian, and A. Kaminski, Nat. Phys. **7**, 21 (2011).
[8] T. Valla, A. V. Fedorov, P. D. Johnson, B. O. Wells, S. L. Hulbert, Q. Li, G. D. Gu, and N. Koshizuka, Science **285**, 2110 (1999).
[9] A. A. Kordyuk, S. V. Borisenko, V. B. Zabolotnyy, J. Geck, M. Knupfer, J. Fink, B. Büchner, C. T. Lin, B. Keimer, H. Berger, A. V. Pan, S. Komiya, and Y. Ando, Phys. Rev. Lett. **97**, 017002 (2006).

[10]W. S. Lee, W. Meevasana, S. Johnston, D. H. Lu, I. M. Vishik, R. G. Moore, H. Eisaki, N. Kaneko, T. P. Devereaux, and Z. X. Shen, Phys. Rev. B **77**, 140504 (2008).
[11]T. Kondo, R. Khasanov, T. Takeuchi, J. Schmalian, and A. Kaminski, Nature (London) **457**, 296 (2009).
[12]J. Graf, C. Jozwiak, C. L. Smallwood, H. Eisaki, R. A. Kaindl, D.-H. Lee, and A. Lanzara, Nat. Phys. **7**, 805 (2011).
[13]I. M. Vishik, M. Hashimoto, R.-H. He, W.-S. Lee, F. Schmitt, D. Lu, R. G. Moore, C. Zhang, W. Meevasana, T. Sasagawa, S. Uchida, K. Fujita, S. Ishida, M. Ishikado, Y. Yoshida, H. Eisaki, Z. Hussain, T. P. Devereaux, and Z.-X. Shen, Proc. Natl. Acad. Sci. (USA) **109**, 18332 (2012).
[14]C. L. Smallwood, C. Jozwiak, W. T. Zhang, and A. Lanzara, Rev. Sci. Instrum. **83**, 123904 (2012).
[15]A. Lanzara, P. V. Bogdanov, X. J. Zhou, S. A. Kellar, D. L. Feng, E. D. Lu, T. Yoshida, H. Eisaki, A. Fujimori, K. Kishio, J.-I. Shimoyama, T. Noda, S. Uchida, Z. Hussain, and Z.-X. Shen, Nature (London) **412**, 510 (2001).
[16]C. L. Smallwood, J. P. Hinton, C. Jozwiak, W. Zhang, J. D. Koralek, H. Eisaki, D.-H. Lee, J. Orenstein, and A. Lanzara, Science **336**, 1137 (2012).
[17]N. Gedik, P. Blake, R. C. Spitzer, J. Orenstein, R. Liang, D. A. Bonn, and W. N. Hardy, Phys. Rev. B **70**, 014504 (2004).
[18]R. A. Kaindl, M. A. Carnahan, D. S. Chemla, S. Oh, and J. N. Eckstein, Phys. Rev. B **72**, 060510 (2005).
[19]G. Coslovich, C. Giannetti, F. Cilento, S. Dal Conte, G. Ferrini, P. Galinetto, M. Greven, H. Eisaki, M. Raichle, R. Liang, A. Damascelli, and F. Parmigiani, Phys. Rev. B **83**, 064519 (2011).
[20]C. L. Smallwood, W. T. Zhang, T. Miller, C. Jozwiak, H. Eisaki, D.-H. Lee, and A. Lanzara (unpublished).
[21]A. Mourachkine, *High-Temperature Superconductivity in Cuprates: The Nonlinear Mechanism and Tunneling Measurements* (Springer, Dordrecht, 2002).
[22]J. Hwang, T. Timusk, and G. D. Gu, J. Phys.: Condens. Matter **19**, 125208 (2007).
[23]D. N. Basov, R. D. Averitt, D. van der Marel, M. Dressel, and K. Haule, Rev. Mod. Phys. **83**, 471 (2011).
[24]M. Oda, K. Hoya, R. Kubota, C. Manabe, N. Momono, T. Nakano, and M. Ido, Physica C **281**, 135 (1997).
[25]U. Chatterjee, D. F. Ai, J. J. Zhao, S. Rosenkranz, A. Kaminski, H. Raffy, Z. Z. Li, K. Kadowaki, M. Randeria, M. R. Norman, and J. C. Campuzano, Proc. Natl. Acad. Sci. (USA) **108**, 9346 (2011).
[26]J. Tanaka, C. Tanaka, K. Takada, and W. Mori, Phys. Status Solidi B **215**, 541 (1999).
[27]C. Meingast, V. Pasler, P. Nagel, A. Rykov, S. Tajima, and P. Olsson, Phys. Rev. Lett. **86**, 1606 (2001).
[28]D. S. Fisher, Phys. Rev. Lett. **56**, 416 (1986).
[29]V. L. Ginzburg, Sov. Phys.: Solid State **2**, 1824 (1960).
[30]Y. Wang, L. Li, and N. P. Ong, Phys. Rev. B **73**, 024510 (2006).
[31]R.-H. He, M. Hashimoto, H. Karapetyan, J. D. Koralek, J. P. Hinton, J. P. Testaud, V. Nathan, Y. Yoshida, H. Yao, K. Tanaka, W. Meevasana, R. G. Moore, D. H. Lu, S.-K. Mo, M. Ishikado, H. Eisaki, Z. Hussain, T. P. Devereaux, S. A. Kivelson, J. Orenstein, A. Kapitulnik, and Z.-X. Shen, Science **331**, 1579 (2011).
[32]K. Ishida, K. Yoshida, T. Mito, Y. Tokunaga, Y. Kitaoka, K. Asayama, A. Nakayama, J. Shimoyama, and K. Kishio, Phys. Rev. B **58**, R5960 (1998).
[33]L. Ozyuzer, J. F. Zasadzinski, K. E. Gray, C. Kendziora, and N. Miyakawa, Europhys. Lett. **58**, 589 (2002).
[34]R. M. Dipasupil, M. Oda, N. Momono, and M. Ido, J. Phys. Soc. Jpn. **71**, 1535 (2002).
[35]K. K. Gomes, A. N. Pasupathy, A. Pushp, S. Ono, Y. Ando, and A. Yazdani, Nature (London) **447**, 569 (2007).
[36]M. Presland, J. Tallon, R. Buckley, R. Liu, and N. Flower, Physica C **176**, 95 (1991).
[37]V. J. Emery, S. A. Kivelson, and O. Zachar, Phys. Rev. B **56**, 6120 (1997).
[38]H. Fu and D.-H. Lee, Phys. Rev. B **74**, 174513 (2006).
[39]P. C. Howell, A. Rosch, and P. J. Hirschfeld, Phys. Rev. Lett. **92**, 037003 (2004).
[40]N. Gedik, M. Langner, J. Orenstein, S. Ono, Y. Abe, and Y. Ando, Phys. Rev. Lett. **95**, 117005 (2005).
[41]R. Cortés, L. Rettig, Y. Yoshida, H. Eisaki, M. Wolf, and U. Bovensiepen, Phys. Rev. Lett. **107**, 097002 (2011).